Astrochemistry VII – Through the Cosmos
from Galaxies to Planets
Proceedings IAU Symposium No. 332, 2017
M. Cunningham, T. Millar & Y. Aikawa, eds.

doi:10.1017/S1743921317006779

Chemistry of the oldest white dwarf planetary systems

Mark A. Hollands[1], Boris T. Gänsicke[1], Detlev Koester[2], Vadim Alekseev[3] and Emma L. Herbert[1]

[1]Department of Physics, University of Warwick, Coventry CV4 7AL, UK
email: M.Hollands@warwick.ac.uk

[2]Institut für Theoretische Physik and Astrophysik, University of Kiel, 24098 Kiel, Germany

[3]St. Petersburg State University, 7/9 Universitetskaya Nab., 199034 St. Petersburg, Russia

Abstract. Almost all stars in the Milky Way, including the Sun, will end their lives as white dwarfs. Their relatively peaceful transition off of the main sequence implies that most of their planetary systems will survive engulfment during the deaths of their host stars. These remnant planetary systems remain detectable for many Gyr through the occasional metal-contamination of the white dwarf photospheres by tidally disrupted planetesimals. Spectral analysis of these "metal-polluted" white dwarfs therefore provides a direct method for measuring the chemical compositions of extrasolar material. Here we present our sample of 230 cool white dwarfs with metal-rich photospheres, explore the diverse range of compositions of the accreted matter, and discuss two extreme systems which have respectively accreted planetesimals consistent with crust-like and core-like planetary material.

Keywords. stars: planetary systems, white dwarfs, abundances

1. Introduction

1.1. *A review of white dwarf properties*

More than 95 % of all main-sequence stars will eventually become white dwarfs after exhausting their supplies of nuclear fuel. Immediately after leaving the AGB, these newly formed white dwarfs have effective temperatures ($T_{\rm eff}$) of several 100 000 K, but with no nuclear processes providing heat, these stellar embers radiate away their thermal energy over the course of billions of years. Cooling models provide a direct way to measure the age of a white dwarf from its mass and $T_{\rm eff}$.

Most of today's white dwarfs are the descendants of A- and F-type main sequence stars ($M_* \simeq 1.5$–$3.0\,{\rm M}_\odot$), resulting in final masses of $\simeq 0.6\,{\rm M}_\odot$, and due to their electron-degenerate structure small radii of $\simeq 0.01\,{\rm R}_\odot$. The moderate mass enclosed within such a small volume leads to immensely high surface gravities, typically of $\log g \simeq 8$ (cgs).

These extreme gravitational fields have an important consequence for the white dwarf structure, as they cause elements to stratify according to their atomic weights, with the lightest elements at the surface and heaviest in the core. Typically $\simeq 99$ % of the white dwarf mass is contained within the electron-degenerate carbon/oxygen core, shrouded by a thin envelope of helium. In most white dwarfs, the outermost layer, $\simeq 0.01$ % by mass, consists of hydrogen.

Because spectroscopy only probes the outermost layer, an optical spectrum of a "normal" white dwarf shows little more than a series of pressure-broadened Balmer lines (figure 1, top). In about one quarter of white dwarfs, all hydrogen is removed in a late shell flash, and hence their spectra consist only of helium lines (figure 1, bottom).

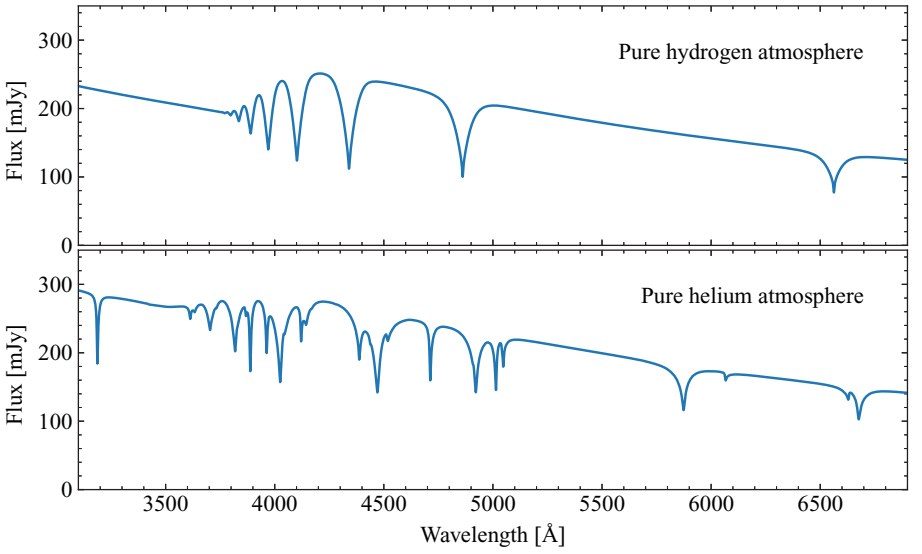

Figure 1. Spectral models for white dwarfs with atmospheres of pure hydrogen and helium. Both models are computed with effective temperatures of 20 000 K and $\log g$ of 8. The fluxes are scaled for white dwarfs observed from a distance of 10 pc. The naive expectation is that all white dwarfs should be observed with similar spectra.

In either case, one thing remains certain: if heavier elements are deposited onto the stellar surface, gravitational settling will cause them to sink below the photosphere on timescales many orders of magnitude shorter than the age of the white dwarf (Paquette *et al.* 1986). For a $T_{\rm eff} = 20\,000$ K white dwarf with a hydrogen atmosphere this process is as short as a few days (Koester 2009). Thus white dwarfs are expected to have pure hydrogen or helium atmospheres. Observationally this could not be further from the truth, with 25–50 % of white dwarfs having metal contaminated atmospheres (Zuckerman *et al.* 2010; Koester *et al.* 2014).

1.2. *Signatures of remnant planetary systems*

Over the last three decades, it has become clear that metals observed in the atmospheres of many white dwarfs, which have been known for a century (van Maanen 1917), signify the presence of remnant planetary systems. An understanding of this relation only began to emerge following observations of the white dwarf G29-38. In the infra-red, an excess of flux (figure 2) was found compared to what was expected if only a white dwarf was present (Zuckerman & Becklin 1987). This was later confirmed to originate from a compact circumstellar disk of dust (Graham *et al.* 1990). Because G29-38 also has a metal lines in its spectrum (Koester *et al.* 1997), it soon became apparent that these observables were connected, where eventually a planetary origin was suggested (Jura 2003).

The accepted scenario is that exoplanetesimals in such systems will sometimes have their orbits perturbed by more massive objects such as a planets (Debes & Sigurdsson 2002). If the perturbation increases the planetesimal eccentricity such that its periastron falls within about 1 $R_\odot$ of the white dwarf, tidal forces will unbind the asteroid (Jura 2003). The resulting dust will then circularise into a debris disk which over time will accrete onto the stellar surface, leading to the appearance of metallic absorption lines in the stellar spectrum.

Spectroscopic observations of G29-38 with Spitzer (Reach *et al.* 2005; Reach *et al.* 2009) have revealed strong 10 μm silicate emission (figure 2) which has been attributed

https://doi.org/10.1017/S1743921317006779 Published online by Cambridge University Press

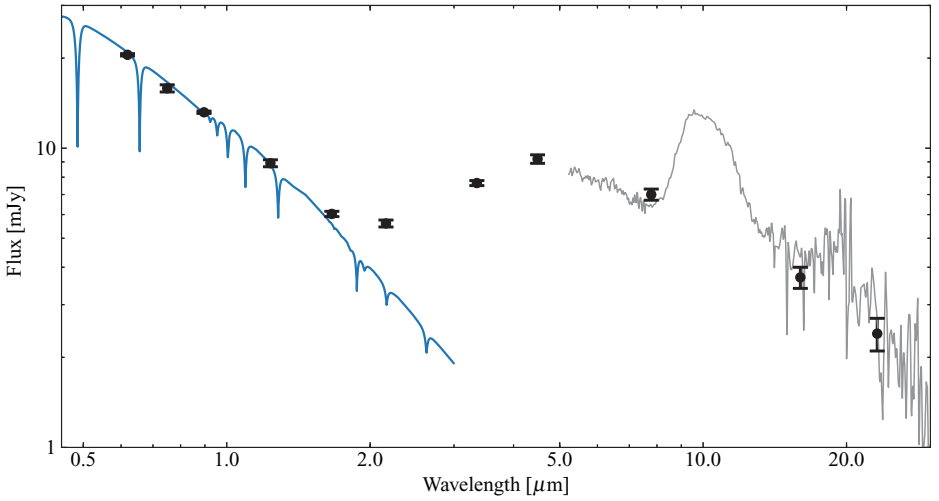

Figure 2. The white dwarf G29-38 exhibits a strong infra-red flux excess beyond about 1.5 μm, above the expected flux of the 12000 K white dwarf model. The Spitzer observations of Reach *et al.* (2005)/ Reach *et al.* (2009) demonstrate unambiguous 10 μm silicate emission. Photometry are from SDSS, APASS, 2MASS, WISE, and Spitzer.

to a mixture of enstatite and forsterite dust grains. While more than forty white dwarfs with circumstellar debris disks are now known from infra-red excesses (Rochetto *et al.* 2015), in addition to G29-38 only one other object (Jura *et al.* 2007) is sufficiently bright enough for spectroscopic follow-up with Spitzer. With JWST available in the near future, it will be possible to detect molecular emission at additional objects, and includes the prospect of carrying out detailed mineralogy in the brightest systems.

The most unambiguous evidence for remnant planetary systems was recently observed at WD 1145+017. This star shows highly variable, deep transits, demonstrating for the first time an asteroid disintegrating in real time (Vanderburg *et al.* 2015; Gaensicke *et al.* 2016). WD 1145+017 also exhibits both an infra-red excess and photospheric metals.

For detailed reviews to remnant planetary systems around white dwarfs, see Jura & Young (2014), Farihi (2016), and Veras (2016).

1.3. *White dwarfs as probes of exoplanetary material*

The otherwise pure hydrogen/helium atmospheres of white dwarfs make them perfect laboratories for analysing the bulk compositions of exoplanetesimals, by accurately measuring the atomic abundance ratios of the accreted material. Of course asteroids are chiefly comprised of molecular species, however the elemental abundance ratios obtained from spectral modeling of the white dwarf can be used to establish the most probable molecules/minerals in the accreted matter, preceding its violent disruption and vaporisation by the white dwarf.

Over the last decade, $\simeq 20$ remnant planetary systems have been analysed in this way. The compositions of the disrupted planetesimals are found to be diverse (Gänsicke *et al.* 2012; Xu *et al.* 2014), indicating a significant fraction of these asteroids are differentiated. For instance the relatively high Ca and Al content found by Zuckerman *et al.* (2011) at NLTT 43806 points to lithospheric material, whereas the enhanced Fe and Ni abundances at Ton 345 found by Wilson *et al.* (2015) are better represented by core-material.

Analysis of two systems have also revealed the accretion of water-rich asteroids (Farihi *et al.* 2013; Raddi *et al.* 2015). In both cases, the oxygen abundances were found to be

https://doi.org/10.1017/S1743921317006779 Published online by Cambridge University Press

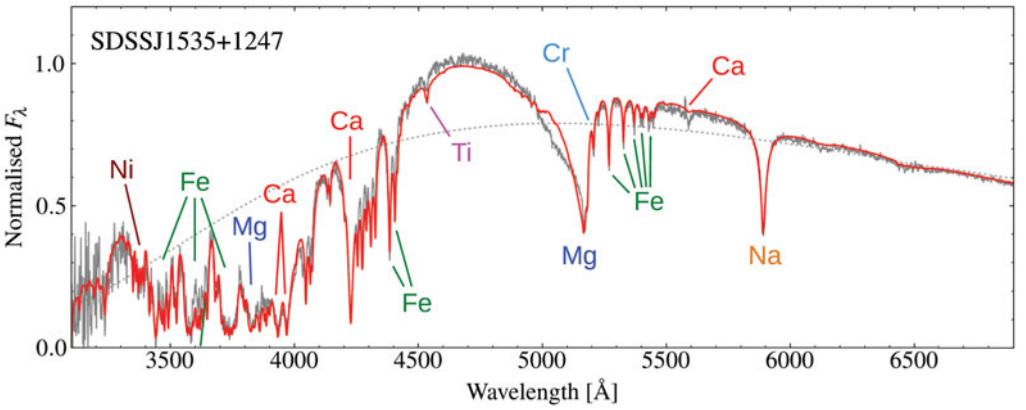

Figure 3. The optical spectrum of the DZ white dwarf SDSS J1535+1247, with its best fitting atmospheric model. The major metal transitions are labelled. A slight discrepancy is seen for the profile of the Mg-b blend (5171 Å), due to the challenge of modelling He-Mg collisions at the high atmospheric densities. The dotted line shows the corresponding model when no metals are present – essentially a blackbody, illustrating how SDSS J1535+1247 will look in a few Myr, once all metals have sunk below the photosphere.

vastly greater than expected from the accretion of minerals containing MgO, SiO_2, CaO etc. (bearing in mind that the dominant rock-forming elements Mg, Al, Si, Ca, and Fe are all easily detected). Because only a fraction of this oxygen could be explained through metal-oxide bearing minerals, and the non-detection of carbon rules out CO and CO_2, the excess oxygen strongly suggest a water-rich origin. In both systems the water mass-fractions of the asteroids were estimated to be a few 10 %, similar to the Solar System asteroid Ceres.

Thus far, all but one of the disrupted planetesimals detected at white dwarfs are consistent with asteroid-like parent bodies. The only exception is, WD 1425+540 which was recently found to have an atmosphere rich in volatile elements including C, N, and S, with an overall abundance pattern similar to the comet Halley, indicating that the white dwarf has accreted a large extrasolar Kuiper-Belt-Object (Xu *et al.* 2017).

2. A large sample of cool white dwarfs with metal-rich photospheres

2.1. *Cool DZ white dwarfs*

Below $T_{\rm eff} \simeq 11\,000$ K, white dwarfs with helium-dominated atmospheres are too cool to show helium transitions. Therefore, if metals have been accreted in sufficient quantities, their lines will be the only transitions observed in their spectra. Such white dwarfs are given the spectral class DZ.

As the $T_{\rm eff}$ is decreased further, helium becomes increasingly transparent and so relatively small traces of metals can have large observational signatures. Therefore, at moderate abundances, DZs often display absorption features from multiple elements, and thus spectroscopic analysis can reveal the composition of the accreted parent body with great accuracy.

Although not the focus of these proceedings, DZs are also old objects having already spent at least 1 Gyr cooling since first becoming a white dwarf. Hence DZs also allow us to study the properties of some of the oldest planetary material in the Milky Way.

Expanding upon the analysis of 26 cool, strongly metal-polluted DZs by Koester *et al.* (2011), we have enlarged this sample to 230 objects making use of spectroscopy available

https://doi.org/10.1017/S1743921317006779 Published online by Cambridge University Press

from the Sloan Digital Sky Survey (SDSS) which we first presented in Hollands *et al.* (2017). The stars in our sample, span a $T_{\rm eff}$ range of 4400–8800 K, with corresponding cooling ages of 1–8 Gyr (white dwarf cooling is non-linear in time), Including the main sequence life time of their progenitors, $\simeq$ 0.5–3.0 Gyr, implies some of these stars are nearly as old as the Galaxy.

The optical spectrum of the brightest DZ we found, SDSS J1535+1247, is shown in figure 3, which in all other regards is typical of the other stars in our sample, including its abundance pattern which is similar to that of the bulk Earth (McDonough 2000). Lines of Ca, Mg, Fe, and Na dominate the spectrum, with Cr, Ti, and Ni also detected owing to the high quality data available for this star. While, Si and O are expected to constitute approximately half of the accreted mass, these elements do not exhibit optical transitions at the low $T_{\rm eff}$ characteristic of DZs.

An important characteristic of the DZs in our sample are the deep convection zones in their outer helium envelopes, which typically comprise 10^{-6} to 10^{-5} of the total white dwarf mass (Hollands *et al.* 2017). Convection severely inhibits metals sinking into the white dwarf interior, with corresponding gravitational settling times of 1–3 Myr. While still significantly shorter than the white dwarf age, this is comparable to, if not longer than the duration of accretion an episode (Girven *et al.* 2012), and so for DZs, accretion-diffusion equilibrium is never reached. Instead the material is mixed throughout the convection zone, and therefore observations of DZs provide lower limits to the mass of the accreted planetesimals, which for our sample range from 10^{20} to 10^{24} g.

2.2. *Distribution of compositions*

Because of the large size of our sample, we are able to statistically explore the variety in exoplanetary material compositions, while also investigating the most interesting systems at a high level of detail (Hollands *et al.* in preparation). Model atmosphere fits to the entire sample yield abundances of Ca, Mg, and Fe for all 230 systems, and Na for around half of objects. Cr, Ti, and Ni are detected in only some systems subject to atmospheric abundances, spectral signal-to-noise, and wavelength coverage.

Considering the sample as a whole, we find that the Fe/Ca atomic abundance ratio provides a simple, but robust indicator of asteroid composition, with low and high Fe/Ca suggesting compositions similar to the Earth's crust and core, respectively. The full distribution of Fe/Ca, seen in Figure 4, spans two orders of magnitude from 1 to 100, where the mean of the distribution in seen to be close to the bulk Earth value of 1.11 (vertical dotted line).

2.3. *Systems exhibiting extreme extrasolar compositions*

In figure 5, we show two systems with high quality spectra from the extremes of the Fe/Ca distribution in figure 4. The atmospheric parameters of these two objects as well as SDSS J1535+1247 (figure 3) are listed in table 1. All three white dwarfs are of similar $T_{\rm eff}$ (5000–6000 K), but due to the variety in accreted material composition, their spectra are all remarkably different.

SDSS J0744+4649 shows an Fe/Ca atomic ratio only slightly above 1, signifying the accretion of a highly differentiated parent body, with a crust-like composition. This is further supported by the clear detections of Ti, and Na, which for the Earth, are both most prominent in the crust. Because crust-material material is largely composed of silicates the combined mass of metals detected from the spectrum likely only amounts to 20 % of the total, with the remaining 80 % contained within undetectable Si and O.

The Fe/Ca ratio for SDSS J0823+0546 is $\simeq$ 100 – despite the meagre abundance, Ca remains well measured from the strong H+K resonance lines. The additional detection of

https://doi.org/10.1017/S1743921317006779 Published online by Cambridge University Press

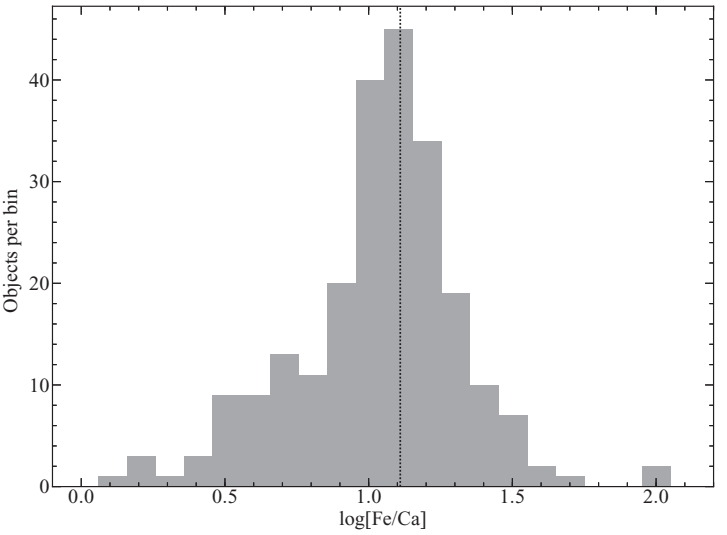

Figure 4. The Fe/Ca distribution for our sample spans two orders of magnitude, demonstrating the huge range in composition for the accreted material. The value for the bulk Earth, which many objects are clustered around, is shown by the dotted vertical line.

Table 1. Results from our fits for the three white dwarfs shown in figures 3 and 5 which we compare with the bulk Earth. In the final row we also list the white dwarf ages. Uncertainties on atomic abundance ratios are all approximately 0.1 dex.

	SDSS J			
	0744+4649	**0823+0546**	**1535+1247**	**Bulk Earth**
$T_{\rm eff}$ (K)	5030 ± 70	6020 ± 60	5770 ± 50	-
log[Ca/He]	-8.36	-9.34	-8.61	-
log[Fe/He]	-8.17	-7.36	-7.57	-
log[Fe/Ca]	$+0.19$	$+1.98$	$+1.04$	$+1.11$
log[Ti/Ca]	-1.02	-	-1.01	-1.37
log[Na/Ca]	-0.90	-	-0.11	-0.68
log[Ni/Fe]	-	-1.23	-1.33	-1.27
Age (Gyr)	$6.4^{+0.4}_{-1.1}$	3.2 ± 0.9	3.8 ± 0.9	-

Ni with Fe/Ni close to the bulk Earth ratio, strongly suggests that this white dwarf accreted a core fragment of a highly differentiated planetesimal. Almost the entire asteroid would have been composed of metallic Fe and Ni, where we estimate these two elements alone comprised at least 80 % of the total asteroid mass. Comparing SDSS J0823+0546 with analyses of similar objects (Wilson *et al.* 2015; Gänsicke *et al.* 2012; Kawka & Vennes 2014), we conclude that this is the most Fe-rich/core-like exoplanetary material detected to date. From the mass of material currently residing in the convection zone of SDSS J0823+0546, we derive a lower limit of $\simeq 4 \times 10^{21}$ g for the total asteroid mass, only one order of magnitude smaller than Psyche, the largest metallic Solar System asteroid (Carry 2012).

3. Conclusions and future work

We have identified a large sample of ancient, metal-rich cool DZ white dwarfs. Analysis of their spectra reveals the compositions of the accreted parent bodies to be extremely diverse, which in some cases are consistent with the accretion of either core or crust material from highly differentiated planetesimals.

https://doi.org/10.1017/S1743921317006779 Published online by Cambridge University Press

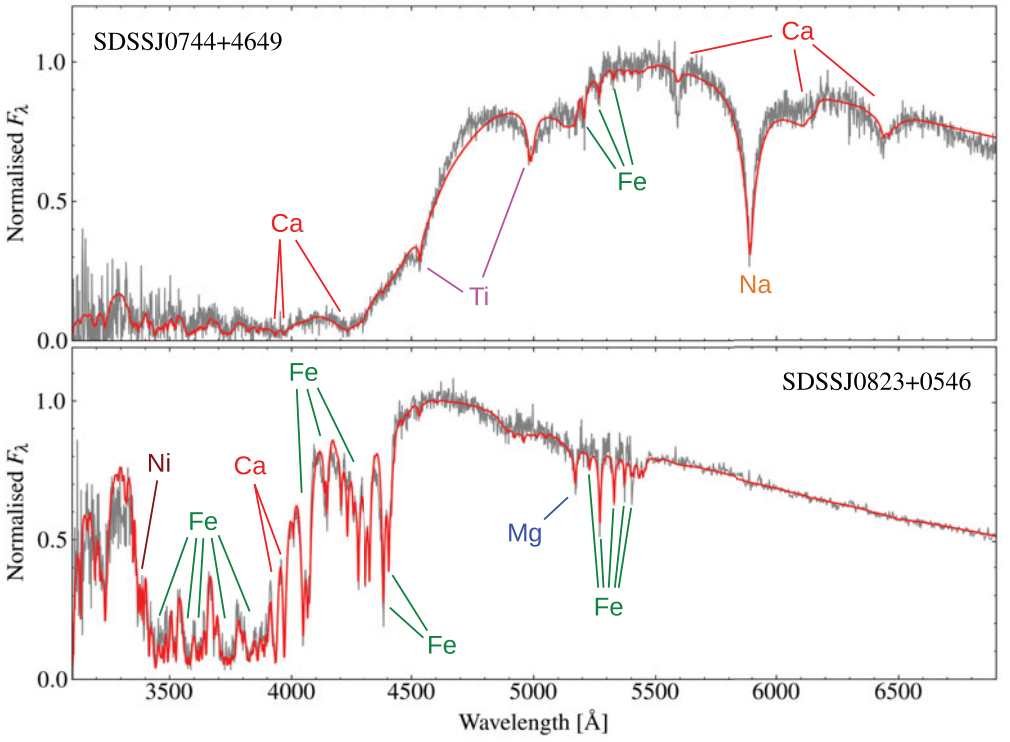

Figure 5. *Top*: SDSS J0744+4649 has a spectrum dominated by elements present in the Earth's crust, i.e. Ca, Ti, and Na. The intense absorption below 4500 Å is due to extreme pressure broadening of the H+K Ca II and 4226 Å Ca I resonance lines. *Bottom*: SDSS J0823+0546 exhibits a plethora of Fe transitions, particularly between 3400-3900 Å. Additionally it shows a blend of Ni lines near 3350 Å indicating the accreted body was rich in core-material.

Many of the objects identified in our sample are expected to appear in the 2nd Gaia data-release. Obtaining parallaxes to these white dwarfs will provide precise constraints on their radii, and in turn accurate estimates of their stellar masses. This will vastly improve the precisions of the white dwarf ages (see table 1) which are currently limited by the unknown stellar masses.

We will then be able to thoroughly investigate the chemistry of remnant planetary systems as a function of Galactic age.

Additional data releases from SDSS and other upcoming spectroscopic surveys will allow us to identify hundreds more metal-contaminated white dwarfs, increasing our understanding on the diversity of remnant planetary systems.

Acknowledgements

The research leading to these results has received funding from the European Research Council under the European Unions Seventh Framework Programme (FP/2007-2013) / ERC Grant Agreement n. 320964 (WDTracer).

References

Carry, B. 2012, *Planet. Space Sci.*, 73, 98

https://doi.org/10.1017/S1743921317006779 Published online by Cambridge University Press

Debes, J. H. & Sigurdsson, S. 2002, *ApJ*, 572, 556
Farihi, J. 2016, *New Astron. Rev.*, 71, 9
Farihi, J., Gänsicke, B. T., & Koester, D. 2013, *Science*, 342, 218
Gänsicke, B. T., Aungwerojwit, A., Marsh, T. R., Dhillon, V. S., Sahman, D. I., Veras, D., Farihi, J., Chote, P., Ashley, R., Arjyotha, S., Rattanasoon, S., Littlefair, S. P., Pollacco, D., & Burleigh, M. R. 2016, *ApJ*, 818, L7
Gänsicke, B. T., Koester, D., Farihi, J., Girven, J., Parsons, S. G., & Breedt, E. 2012, *MNRAS*, 424, 333
Girven, J., Brinkworth, C. S., Farihi, J., Gänsicke, B. T., Hoard, D. W., Marsh, T. R., & Koester, D. 2012, *ApJ*, 749, 154
Graham, J. R., Matthews, K., Neugebauer, G., & Soifer, B. T. 1990, *ApJ*, 357, 216
Hollands, M. A., Koester, D., Alekseev, V., Herbert, E. L., & Gänsicke, B. T. 2017, *MNRAS*, 467, 4970
Jura, M. 2003, *ApJ Lett.*, 584, L91
Jura, M., Farihi, J., Zuckerman, B., & Becklin, E. E. 2007, *AJ*, 133, 1927
Jura, M. & Young, E. D. 2014, *Annual Review of Earth and Planetary Sciences*, 42, 45
Kawka, A. & Vennes, S. 2014, *MNRAS*, 439, L90
Koester, D. 2009, *A&A*, 498, 517
Koester, D., Gänsicke, B. T., & Farihi, J. 2014, *A&A*, 566, A34
Koester, D., Girven, J., Gänsicke, B. T., & Dufour, P. 2011, *A&A*, 530, A114
Koester, D., Provencal, J., & Shipman, H. L. 1997, *A&A*, 320, L57
McDonough, W. 2000, *Earthquake Thermodynamics and Phase Transformation in the Earth's Interior*, Elsevier Science Academic Press, pages 5–24
Paquette, C., Pelletier, C., Fontaine, G., & Michaud, G. 1986, 61, 197
Raddi, R., Gänsicke, B. T., Koester, D., Farihi, J., Hermes, J. J., Scaringi, S., Breedt, E., & Girven, J. 2015, *MNRAS*, 450, 2083
Reach, W. T., Kuchner, M. J., von Hippel, T., Burrows, A., Mullally, F., Kilic, M., & Winget, D. E. 2005, *ApJ Lett.*, 635, L161
Reach, W. T., Lisse, C., von Hippel, T., & Mullally, F. 2009, *ApJ*, 693, 697
Rocchetto, M., Farihi, J., Gänsicke, B. T., & Bergfors, C. 2015, *MNRAS*, 449, 574
van Maanen, A. 1917, *PASP*, 29, 258
Vanderburg, A., Johnson, J. A., Rappaport, S., Bieryla, A., Irwin, J., Lewis, J. A., Kipping, D., Brown, W. R., Dufour, P., Ciardi, D. R., Angus, R., Schaefer, L., Latham, D. W., Charbonneau, D., Beichman, C., Eastman, J., McCrady, N., Wittenmyer, R. A., & Wright, J. T. 2015, *Nat*, 526, 546
Veras, D. 2016, *Royal Society Open Science*, 3, 150571
Wilson, D. J., Gänsicke, B. T., Koester, D., Toloza, O., Pala, A. F., Breedt, E., & Parsons, S. G. 2015, *MNRAS*, 451, 3237
Xu, S., Jura, M., Koester, D., Klein, B., & Zuckerman, B. 2014, *ApJ*, 783, 79
Xu, S., Zuckerman, B., Dufour, P., Young, E. D., Klein, B., & Jura, M. 2017, *ApJ Lett.*, 836, L7
Zuckerman, B. & Becklin, E. E. 1987, *Nat*, 330, 138
Zuckerman, B., Koester, D., Dufour, P., Melis, C., Klein, B., & Jura, M. 2011, *ApJ*, 739, 101
Zuckerman, B., Melis, C., Klein, B., Koester, D., & Jura, M. 2010, *ApJ*, 722, 725